ADVANCED DIAGNOSTICS TO RESOLVE LONG-LASTING CONTROVERSIES IN BOILING HEAT TRANSFER

Matteo Bucci
Assistant Professor, Department of Nuclear Science and Engineering,
Massachusetts Institute of Technology,
Cambridge, MA, 02139,
United States of America,
E-mail: mbucci@mit.edu

ABSTRACT

Boiling heat transfer has been investigated for several decades, but still there are many open questions and controversies about the mechanisms associated with this process and particularly its limit, known as critical heat flux (CHF). This lack of understanding often arose from the absence of experimental capabilities to perform measurements at the space and time scales characteristic of these phenomena. However, improvements have been possible in the last decade thanks to the rapid development of InfraRed (IR) thermometry diagnostics to measure temperature distributions on the boiling surface [1-13].

In this work, we discuss first-of-a-kind investigations enabled by advanced IR diagnostics developed in the Nuclear Science and Engineering (NSE) department at the Massachusetts Institute of Technology (MIT). Specifically, a new technique has been developed [14], requiring the solution of a couple conduction/radiation inverse problem, to measure temperature and heat flux distributions on the boiling surface with a space resolution of approximately 100 μm, and frame rates from 2500 to 4000 fps. This technique is being leveraged to shed light on many phenomena still debated within the boiling heat transfer community. The list of controversial issues addressed in this talk includes but is not limited to: CHF in steady-state [15] and transient conditions, such as power escalations; onset of nucleate boiling (ONB) temperature in steady-state and transient conditions [16,17]; and CHF enhancement on micro- and nano-engineered surfaces. Here, a specific controversy is addressed, about the partition of the wall heat flux in flow boiling heat transfer.

INTRODUCTION

Mechanistic models for the prediction of heat transfer coefficients in boiling heat transfer rely on the so-called wall heat partitioning approach, where the total heat flux transferred at the boiling wall is represented as the sum of several contributions associated with different heat transfer mechanisms. Traditional models have been adapted from the original heat partitioning formulation proposed by Judd and Hwang [18] and adopted by Kurul and Podowski[19] for pool boiling conditions. As such, they consist of three contributions: evaporation, quenching and single-phase convection. More recently, Basu et al. [20], Yeoh et al. [21] and Gilman and Baglietto [22] introduced a further contributions observed in flow boiling conditions, associated with the sliding of bubbles on the boiling surface. However, due to a lack of experimental capabilities to provide a direct measurement of heat flux partitioning, only indirect validation has been possible, using integral quantities such as the heat transfer coefficient and wall superheat. Surprisingly, these models can predict consistent heat transfer coefficient and superheat using different heat partitioning schemes [23]. Precisely, there is a significant difference in the evaporation term, which results in different vapor production rates. To date, no clear consensus on the weight of the different terms has been achieved. Very little work has been done to experimentally capture flow boiling phenomena at the resolutions needed for the validation of these models. To this end, we present here a first-of-a-kind experiment for capturing subcooled flow boiling data, including unique measurements of the wall heat flux partitioning.

EXPERIMENTAL METHODS

The Platform for Experimental ThERmal-hydraulics (PEThER) is a flow-boiling loop designed, constructed and operated at MIT. The whole loop is built with stainless steel 316L and is designed for operation with DI-water up to 10 bar at saturation conditions and mass fluxes as large as 2500 kg/m^{2}s. At the heart of the facility is a test section (see Figure1) with a 3cm × 1cm flow channel running the length of the structure. The test section connects to an entrance region providing more than 60 L/D to establish fully-developed turbulent flow. The main body of the test section consists of four sides, three are used for quartz windows to provide high-speed video (HSV) optical access, the fourth wall contains the cartridge used to hold an InfraRed (IR) heater. The cartridge is made of a ceramic material called Shapal, which is electrically insulating and mechanically strong enough to act as a pressure boundary. The IR heater (see Figure 2) is installed inside the cartridge. It consists of a sapphire substrate coated with indium-tin-oxide (ITO). The sapphire substrate is a 20×20 mm^2 slide, 1 mm thick. The ITO coating, in contact with water, is wrapped around the substrate and serves as a Joule heater. The ITO is nano-smooth, but has localized imperfections in the range of a few microns. It has a thickness of 0.7 μm and a resistivity of 2.5 Ω/square. Silver pads are deposited on top of the ITO and wrap around the filleted edges

of the sapphire substrate. They limit the active ITO area to a 10×10 mm^2 square and allow a uniform supply of electric power to the heater surface. The ITO coating is opaque in the 3-5 μm wavelength range and transparent in the visible light wavelengths. Sapphire is instead quasi-transparent to the infrared radiation emitted by the ITO and transparent to the visible light. This allows a high-speed video camera (Phantom v12.1, operated at 10000 frames per second) to image the heater from the front and the side (see Figure 3), while simultaneously allowing a synchronized IR camera (IRCameras 806HS, operated at 2500 frames per second) to image the ITO coating through the sapphire and to collect data on the temperature and heat flux according to the algorithm described in [14]. Precisely, due to the slightly absorbing nature of sapphire, the post-processing of the IR images requires the solution of a coupled conduction-radiation inverse problem. The typical output of an experiment is the time-dependent 2-D surface temperature and corresponding heat flux distributions on the boiling surface, as shown in Figure 4 and Figure 5, respectively.

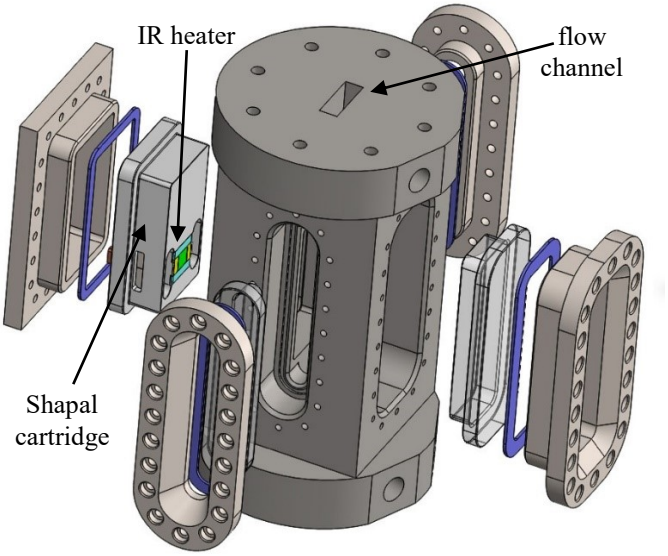

Figure 1 Exploded view of the flow boiling test section

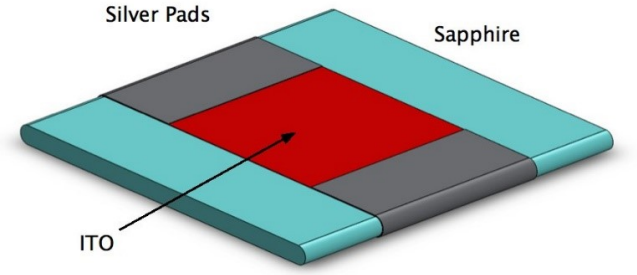

Figure 2 IR heater (20×20 mm^2, 1 mm thick) consisting of a sapphire substrate, electrically-conductive, IR-opaque ITO coating acting as Joule heater and silver pads

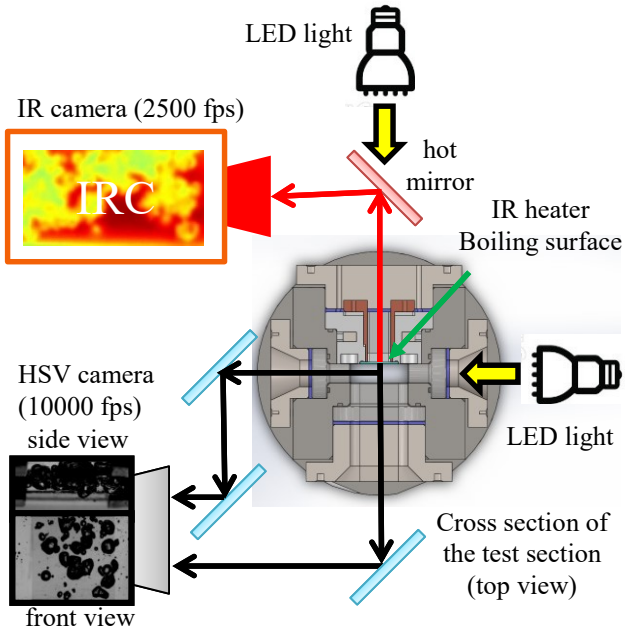

Figure 3 Optical arrangement

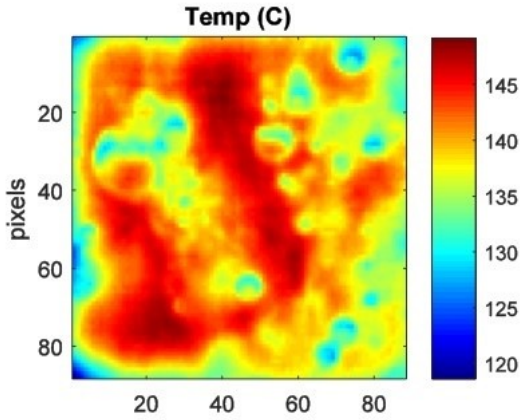

Figure 4 Typical temperature distribution on the boiling surface (each pixel corresponds to 115×115 μm^2)

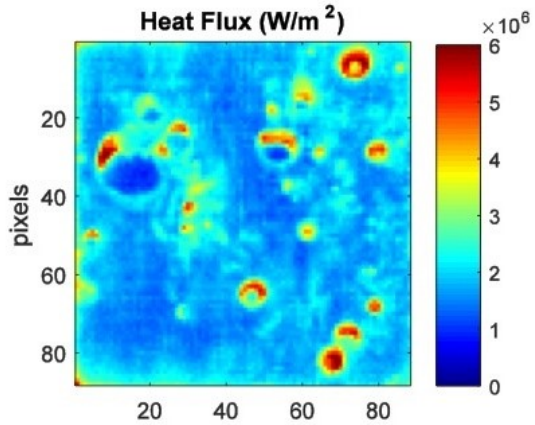

Figure 5 Typical heat flux distribution on the boiling surface (each pixel corresponds to 115×115 μm^2)

DISCUSSION

From time-dependent temperature and heat flux distributions it is possible to measure fundamental quantities such as average temperature and heat flux to obtain the boiling curves, nucleation site density, bubble departure frequency, wait time and growth time, dry area fraction and contact line density. More importantly, it is possible to estimate the contribution of evaporation and the other terms of the wall heat partitioning. This goal is achieved using a specific image processing procedure, as explained next. Regions where the liquid is evaporating have the higher heat flux values and appear as red, yellow and greenish areas in Figure 5. However, the heat flux in quenching heat transfer can also be very high and therefore it is not accurate to distinguish between evaporation and quenching basing solely on the heat flux level. In order to improve the detection of the evaporation areas, the heat flux distribution was pre-processed leveraging the front-view images recorded by the HSV camera. An example is provided in Figure 6. At each step, the heat flux distribution (left) is masked with the HSV image (center).

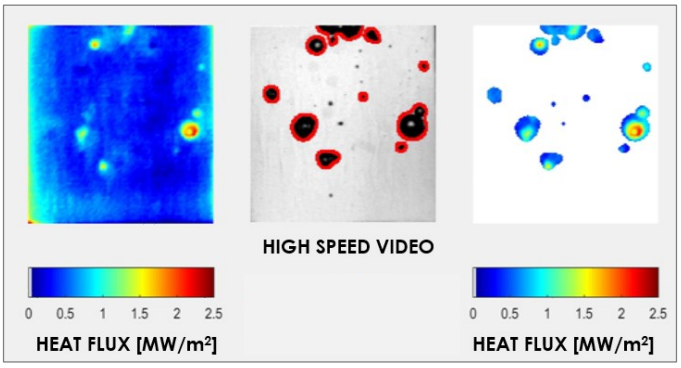

Figure 6 Example of image pre-processing for the detection of the evaporation heat transfer areas

Areas where bubbles are not present are automatically discarded, as shown in Figure 6 (right). Then, a filter based on the heat flux level is applied to distinguish between areas where evaporation is actually occurring from regions where the bubbles are not in contact with the surface and heat transfer occurs without mass transfer. Figure 7 shows the heat flux partitioning for flow boiling test run at atmospheric pressure with a subcooling of 10K and a mass flux of 500 kg/m^{2}s. The black dots represent heat transfer in the dry area regions, where the surface is in contact with vapor. This term is measured as the time-average of

$$\frac{q''_{dry}(t)}{q''_{avg}} = \frac{1}{A_{tot}} \int_{A_{dry}(t)} q''(x,y,t)\, dA \qquad (1)$$

where A_{dry} is the dry area, A_{tot} is the total heater area (1 cm^2), q''_{avg} is the surface average heat flux and x and y are the coordinates on the surface. Not surprisingly, the heat flux through the dry areas is very small. The evaporation term (red dots), measured similarly, increases significantly with the heat flux. This is consistent with the increase of the nucleation site density and the bubble departure frequency. However, the contribution of evaporation never exceeds 50%, the value measured at CHF. The green dots, labelled q_{sp}, represent the complement to the evaporation and the dry area heat transfer terms. They include both the single-phase forced convection and quenching heat transfer terms associated with bubble departure or sliding. An attempt to separate these two terms has been made in similarity with the modelling strategy often adopted in heat partitioning models, as explained next. First, the single phase forced convection coefficient h_{fc} has been measured at low heat fluxes, with no boiling occurring on the surface. Then, for each frame, the single-phase heat transfer area A_{sp} has been obtained as the complement to the evaporation and the dry areas. Finally, the single-phase forced convection heat transfer term (blue points in Figure 7) has been quantified as the time average of

$$\frac{q''_{fc}(t)}{q''_{avg}} = \frac{1}{A_{tot}} \int_{A_{sp}} h_{fc}\,(T_w(x,y,t) - T_b)\, dA \qquad (2)$$

where T_w is the measured surface temperature and T_b is the fluid bulk temperature. Here we assumed that the forced convection flow and its heat transfer coefficient are not affected by the presence of the bubbles. However, bubbles can cause local modifications of the flow field, e.g. acceleration, or enhance the turbulence of single-phase momentum boundary layer. With these assumptions, the quenching term, q_q has been estimated as the difference between the single phase term (green dots) and the forced convection term (light blue dots). It represents the heat transfer enhancement due to quenching phenomena associated with bubble departure and sliding. Also, the forced convection term decreases monotonically, as expected according to mechanistic boiling heat transfer models. Interestingly, the quenching term first increases in similarity with the evaporation term, due to the increase of the bubble nucleation frequency and the nucleation site density, but then reaches a maximum and decreases as the average heat flux approaches CHF conditions.

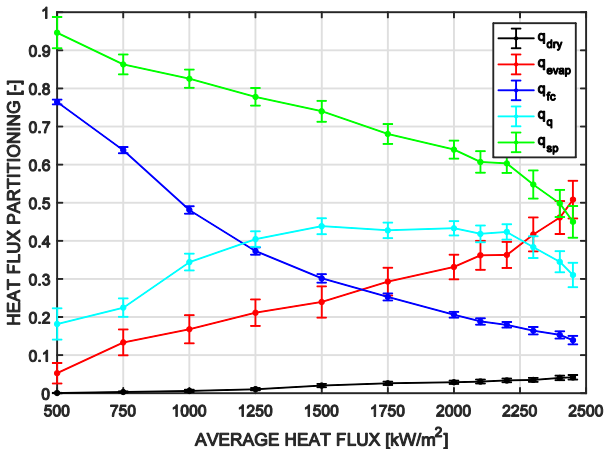

Figure 7 Partitioning of the wall heat flux as a function of the average heat flux for flow boiling test run at atmospheric pressure with a subcooling of 10K and a mass flux of 500 kg/m^{2}s

Results like those shown in Figure 7 provide a comprehensive database for benchmarking and selecting wall heat partitioning models. Moreover, the unique insight provided by all the

measurements enabled by this experimental technique is key to achieving a better understanding of these and many other phenomena, and developing better mechanistic models.

REFERENCES

[1] I. Golobic, J. Petkovsek, M. Baselj, A. Papez, D. Kenning, Experimental determination of transient wall temperature distributions close to growing vapor bubbles, Heat Mass Transfer 45 (2009) 857-866.

[2] N. Schweizer, P. Stephan, Experimental study of bubble behavior and local heat flux in pool boiling under variable gravitational conditions, Multiphase Sci. Technol. 21 (2009) 329-350.

[3] I. Golobic, J. Petkovsek, D.B.R. Kenning, Bubble growth and horizontal coalescence in saturated pool boiling on a titanium foil, investigated by high-speed IR thermography, Int. J. Heat. Mass Tran 55 (2012) 1385-1402.

[4] T.G. Theofanous, J.P. Tu, A.T. Dinh, T.N. Dinh, The boiling crisis phenomenon - Part I: nucleation and nucleate boiling heat transfer, Exp. Therm. Fluid Sci. 26 (2002) 775-792.

[5] T.G. Theofanous, T.N. Dinh, J.P. Tu, A.T. Dinh, The boiling crisis phenomenon - Part II: dryout dynamics and burnout, Exp. Therm. Fluid Sci. 26 (2002) 793-810.

[6] S. Fischer, S. Herbert, A. Sielaff, E.M. Slomsky, P. Stephan, M. Oechsner, Experimental investigation of nucleate boiling on a thermal capacitive heater under variable gravity conditions, Microgravity Sci. Tech. 24 (2012) 139-146.

[7] P. Stephan, A. Sielaff, S. Fischer, J. Dietl, S. Herbert, A contribution to the basic understanding of nucleate boiling phenomena: generic experiments and numeric simulations, Thermal Science and Engineering 21 (2013) 39-57.

[8] C. Gerardi, J. Buongiorno, L.W. Hu, T. McKrell, Study of bubble growth in water pool boiling through synchronized, infrared thermometry and high-speed video, Int. J. Heat. Mass Tran 53 (2010) 4185-4192.

[9] X. Duan, B. Phillips, T. McKrell, J. Buongiorno, Synchronized high speed video, infrared thermometry and PIV data for validation of interface-tracking simulations of nucleate boiling phenomena, Experimental heat transfer 26 (2012) 169-197.

[10] S. Jung, H. Kim, An experimental method to simultaneously measure the dynamics and heat transfer associated with a single bubble during nucleate boiling on a horizontal surface, Int. J. Heat Mass Transfer 73 (2014) 365-375.

[11] B. Phillips, Experimental Investigation of Subcooled Flow Boiling Using Synchronized High Speed Video, Infrared Thermography, and Particle Image Velocimetry, PhD Thesis, Massachusetts institute of Technology, Cambridge, MA, 2014.

[12] J. Yoo, C.E. Estrada-Perez, Y.A. Hassan, An accurate wall temperature measurement using infrared thermometry with enhanced two-phase flow visualization in a convective boiling system, Int. J. Thermal Science 90 (2015) 248-266.

[13] T.H. Kim, E. Kommer, S. Dessiatoun, J. Kim, Measurement of two-phase flow and heat transfer parameters using infrared thermometry, Int. J. Multiphase Flow 40 (2012) 56-67.

[14] M. Bucci, A. Richenderfer, G.-Y. Su, T. McKrell and J. Buongiorno, A mechanistic IR calibration technique for boiling heat transfer investigations, International Journal of Multiphase Flow, vol. 83, pp. 115-127, 2016.

[15] A. Richenderfer, A. Kossolapov, M. Bucci, T. McKrell and J. Buongiorno, IR-thermography-based investigation of critical heat flux in subcooled flow boiling of water at atmospheric conditions, Technical report, CASL Technical Report, 2016.

[16] G.-Y. Su, M. Bucci, T. McKrell and J. Buongiorno, Transient boiling heat transfer of water under exponential heat inputs. Part I: pool boiling, International Journal of Heat and Mass Transfer, vol. 96, p. 667-684, 2016.

[17] G.-Y. Su, M. Bucci, T. McKrell and J. Buongiorno, Transient boiling heat transfer of water under exponential heat inputs. Part II: flow boiling, International Journal of Heat and Mass Transfer, vol. 96, p. 685–698, 2016.

[18] R. L. Judd and K. Hwang, A comprehensive model for nucleate pool boiling heat transfer including microlayer evaporation, Journal of Heat Transfer, vol. 98, no. 4, pp. 623-629, 1976.

[19] N. Kurul and M. Z. Podowski, Multidimensional effects in forced convection subcooled boiling, in Proceedings of the 9th International Heat Transfer Conference, Jerusalem, 1990.

[20] N. Basu, G. R. Warrier and D. V. K., Wall heat flux partitioning during subcooled flow boiling: Part 1 - model development, Journal of Heat Transfer, vol. 127, pp. 131-140, 2005.

[21] G. Yeoh, S. Vahaji, S. Cheung and J. Tu, Modeling subcooled flow boiling in vertical channels at low pressures - part 2: Evaluation and mechanistic approach, Int. J. Heat and Mass Transfer, vol. 75, p. 754–768, 2014.

[22] L. Gilman and E. Baglietto, Advances on wall boiling modelling in CFD: leveraging new understanding from the MIT flow boiling facility, in Proceedings of the 15th International Topical Meeting on Nuclear Reactor Thermal-Hydraulics, Pisa, 2013.

[23] E. Baglietto, M. Christon, Demonstration & assessment of advanced modeling capabilities to multiphase flow with sub-cooled boiling, Technical report, CASL Technical Report: CASL-U-2013-0181- 001, 2013.